Radiation Protection Dosimetry (2012), Vol. 150, No. 4, pp. 474–487
Advance Access publication 28 November 2011
doi:10.1093/rpd/ncr436

DISTRIBUTION OF NATURAL RADIOACTIVITY IN SEDIMENT CORES FROM AMVRAKIKOS GULF (WESTERN GREECE) AS A PART OF IAEA'S CAMPAIGN IN THE ADRIATIC AND IONIAN SEAS

C. Tsabaris[1,*], N. Evangeliou[2], E. Fillis-Tsirakis[1], M. Sotiropoulou[2], D. L. Patiris[1] and H. Florou[2]
[1]Hellenic Centre for Marine Research, Institute of Oceanography, 46.7 Km Athens-Sounio Avenue, PO Box 712, Anavyssos 19013, Greece
[2]National Centre for Scientific Research 'Demokritos', Institute of Nuclear Technology and Radiation Protection, Environmental Radioactivity Laboratory, Athens 153 10, Greece

*Corresponding author: tsabaris@ath.hcmr.gr

Received March 22 2011, revised July 20 2011, accepted October 24 2011

The vertical distribution of natural radionuclides (^{232}Th decay, ^{238}U decay, ^{40}K and ^{210}Pb) was assessed in sediment cores collected from the Amvrakikos Gulf, (Ionian Sea, Western Greece). Two collection stations were selected, the first at the western part of the Gulf near Preveza Strait (13A station) and the other near the centre of the Gulf (13B station). Activity concentrations were measured by means of gamma-ray spectrometry using high-purity germanium (HPGe) detectors installed at two national laboratories. The activity concentration of ^{226}Ra was found in a range from 10 to 20 Bq kg^{-1}, while the activity concentration of ^{222}Rn daughters (^{214}Pb, ^{214}Bi) ranged from 6 to 20 Bq kg^{-1}. The activity concentration of ^{228}Ac varied from 20 to 28 Bq kg^{-1}, while ^{220}Rn daughters (^{212}Pb, ^{208}Tl) from 7 to 35 Bq kg^{-1}. As concerns ^{40}K and ^{210}Pb, their activities varied from 400 to 830 Bq kg^{-1} and from 11 to 360 Bq kg^{-1}, respectively. Also, the data of ^{210}Pb were utilised in the calculations of the sedimentation rate along the sediment cores. Both locations were characterised by a consistent pattern with the average rates of 0.55 $\pm$ 0.02 and 0.32 $\pm$ 0.02 cm y^{-1}, corresponding to 13A and 13B stations, respectively. Finally, the measurements constituted the basis of the first reported database concerning the radiological condition of the Gulf and which can be reclaimed as reference values in future monitoring studies.

INTRODUCTION

Measurements of natural radioactivity in aquatic-sedimentary environments have been of significant importance in studies related to marine pollution and sedimentary processes. The sediment plays an important role in aquatic ecosystems and so monitoring radiological studies might lead to better management and protection of marine resources[(1)]. Semi-closed and closed marine ecosystems act as deposition areas for washed-out materials due to human activities occurring around the catchment area. Those materials include radionuclide contaminants due to naturally occurring radioactive materials (NORM) and/or technologically enhanced NORM (TENORM)[(2)]. Recent studies have been published investigating the distribution of natural radionuclides in the bottom sediments. At Burulus Lake (Egypt), natural radionuclides have been used as tracers to investigate their pathways and mechanisms of mobility, as well as to indicate and assess the radiological impact of pollution[(3)]. In the Gulf of Aqaba (Red Sea), core and beach sediments were studied for radio-ecological purposes by measuring the levels of natural radioactivity due to human activities relevant to the exportation of phosphate ore[(4)]. At Butrint Lake (Albania), superficial sediments were also measured for seabed characterisation and correlation with the granulometry data[(5)].

In general, most studies focus on the activity concentration of the primordial series products (^{238}U and ^{232}Th daughters) and on the concentration of radioactive potassium ^{40}K. Usually, activity concentrations of ^{238}U, ^{232}Th daughters are associated with heavy minerals, and ^{40}K activity concentrations with clay minerals[(6)]. Also, particular interest is given to ^{210}Pb as it is the most long-lived daughter of the inert radioactive gas radon ^{222}Rn. Enhanced activity concentration of ^{210}Pb may be observed in lakes and gulfs as a result of the physical accumulation process relevant to the water cycle. Lead is transported from terrestrial regions into the atmosphere via ^{222}Rn diffusion and during rainfalls it may be accumulated in closed ecosystems as a result of scavenging from raindrops. Additionally, lead ^{210}Pb and radium could be transported from industrial regions and/or agricultural areas by disposal of TENORM materials into rivers where their estuaries are located in the closed systems.

The Amvrakikos Gulf (Western Greece) is a semi-closed ecosystem connected via the narrow Preveza strait with the Ionian Sea. Two rivers (the Arachthos and the Louros) are discharged into the gulf. Due to

extended agricultural activities in the area, the Gulf's water and sediment are constantly enriched by agricultural residues. As the gulf is a protected area according to the Ramsar Convention (1971), surveys have been performed evaluating the condition of the Gulf's ecosystem[7–9]. As a general conclusion those studies reveal potential hazards for the gulf's ecosystem due to increased levels of chemical and biological substances (e.g. nutrients, chlorophyll *a*) in combination with dysoxic/anoxic conditions in water and sediment.

Despite the aforementioned studies, no published information is available regarding the radioactivity levels of the Amvrakikos Gulf. So, as part of the IAEA's campaign in the Adriatic and Ionian seas, this work aims to provide a first radiological study concerning the levels of natural radioactivity and a baseline database for this semi-closed ecosystem. The activity concentration levels of gamma-ray emitting radionuclides in the sediment cores were estimated and subsequently were compared with data from similar marine ecosystems. The database obtained from this work could be used as a baseline in future long-term monitoring studies according to IAEA guidelines for NORM and TENORM monitoring programmes.

STUDY AREA

The Amvrakikos Gulf (Figure 1) is a semi-closed dilution basin of 405 km^2 that receives nutrient inputs, fresh water and sediment fluxes, from a drainage basin of 3850 km^2 (including the catchments of the rivers Arachthos and Louros)[10]. Specifically, the Louros contributes with a drainage basin of 865 km^2 and provides a mean annual water flux of 600×10^6 m^3 y^{-1}, whereas the Arachthos contributes with 1900 km^2 and 2200×10^6 m^3 y^{-1}[11]. In addition, the Gulf receives annually, through precipitation (900–1100 mm y^{-1}), a volume of fresh water of $\sim 400 \times 10^6$ m^3. It comprises relatively shallow depths (a maximum depth of 65 m in the eastern part) and communicates with the open Ionian Sea through a narrow channel (~600 m wide and 5 m depth). The northern part of the Gulf is rather shallow and consists of a relatively wide subaqueous delta/prodelta platform (1–3 km wide), created by the deposition of sediments from the two main rivers, the Arachthos and the Louros.

The major terrestrial sediment fluxes are associated with the main rivers, with the River Arachthos being the most important sediment source, as it annually transports 7.31×10^6 tonnes of suspended sediment[12]; as such, it is among the Mediterranean rivers with the highest annual sediment yield (3890 tonnes km^{-2}). The suspended sediment load of the Louros River is low ($<0.5 \times 10^6$ tonnes y^{-1})[12]. Similarly, the contribution of coastal erosion is expected to be very small, due to the rather weak wave activity in response to small wave fetches (<30 km).

The Gulf presents a two-layer water stratification, characterised by a minimum depth of ~5 m, with the upper layer occupying the first 10 m (with the exception of summer when it is extended up to 20 m) and the lower layer being rather homogenous[13]. The seasonal variations of temperature (T) and salinity (S) are apparent in the Gulf compared with those of the open Ionian Sea, attributed to the difference between fresh water input (riverine flux and precipitation) and evaporation.

The tidal values are <20 cm[14], characterised by a relatively calm wave regime due to the limited wave fetches[15]. Surface water circulation is also weak, presenting a clockwise trend[16]. Measured current speeds in the central part of the Gulf demonstrate mean values ranging from 0.3 up to 0.19 m s^{-1} (in winter)[13]. The same authors have reported fast currents in the Strait of Preveza, ranging from 0.12 to 0.15 m s^{-1} with some bursts reaching 1 m s^{-1}.

The upper water layer in the Gulf is well oxygenated, with dissolved oxygen (DO) levels being >7 ppm. In contrast, the lower layer had values >3 ppm during spring and <1 ppm in summer. Moreover, in a water depth of >40 m and closer to the seabed, the DO was ≤0.3 ppm, indicating the development of anoxic conditions, at least during the summer period. This pattern is attributed to the strong stratification of the waters, which inhibits the renewal of deeper water masses[17].

Inter-seasonal measurements have revealed the eutrophic character of the Gulf (in particular of the Preveza Bay) relative to the surface waters of the adjacent open Ionian Sea. The increased nutrient concentrations are also related to high values of chlorophyll *a*, with the highest values in spring (22.0–44.8 mg l^{-1}) and the lowest during the summer and autumn periods (0.3–1.8 mg l^{-1})[18]. For comparison, chlorophyll *a* levels in the Ionian Sea are <0.7 mg l^{-1}, throughout the year[19].

Two sampling positions were selected for this work. The first one, named 13A, is located close to the Preveza straits and the second, named 13B, near the centre of the Gulf. The first position was selected in order to investigate potential interactions (e.g. seawater and/or sediment exchange) with the Ionian Sea and the second as it is strongly affected by the river estuaries from the north part of the gulf (the Archos and Louros rivers).

MATERIALS AND METHODS

A sampling cruise was carried out as a part of the International Atomic Energy Agency's (IAEA) project RER/7/003, International Scientific Cruise to Adriatic and Ionian Seas, held within 17–28

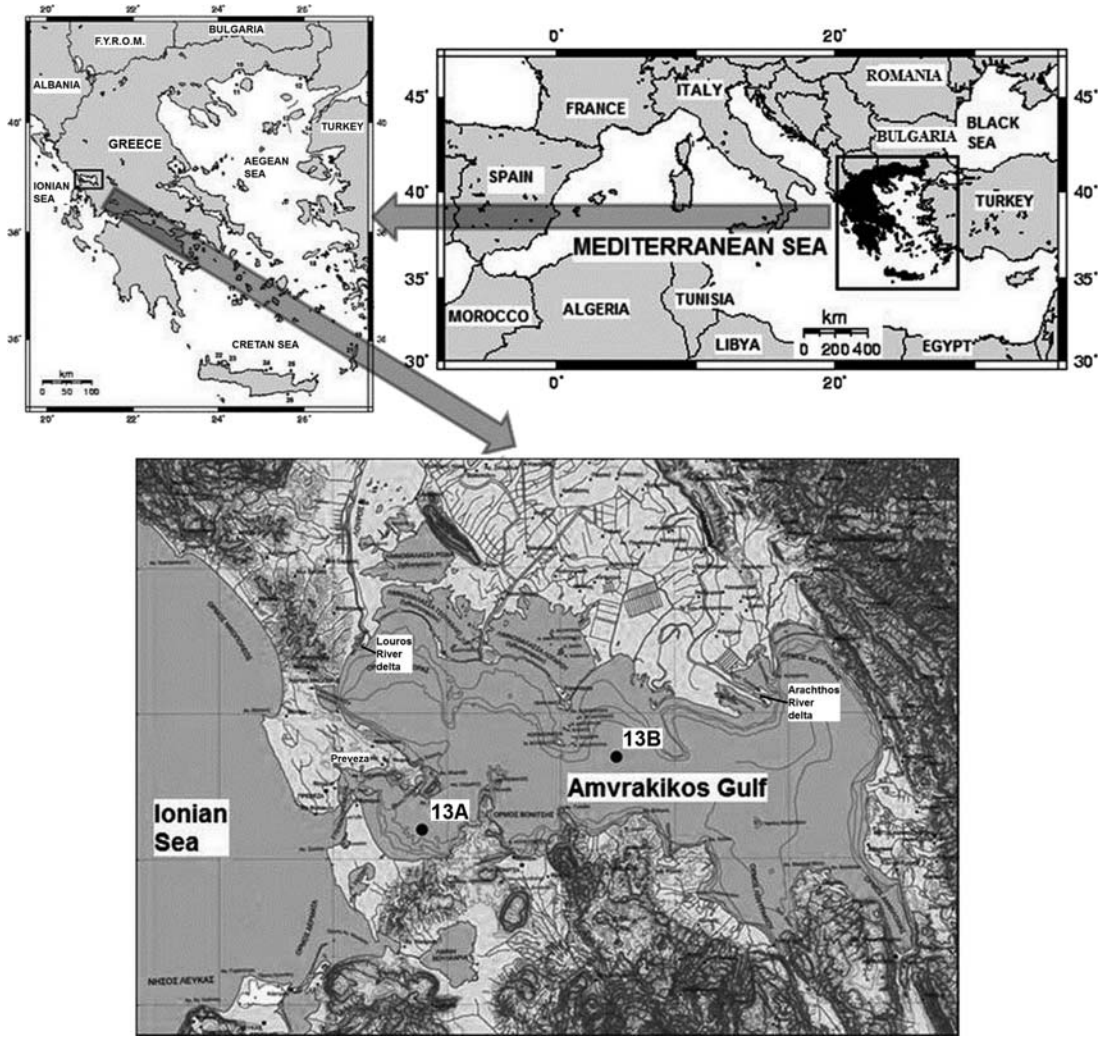

Figure 1. Study area.

September 2007. Sediment core samples were collected using a Bowers and Connelly, Mark VI multicorer analyser [20]. The samples were transferred to the Marine Environment Laboratories of IAEA in Monaco for recording the procedure and then supplied to the laboratories involved.

The analyses were carried out in the Laboratory of Marine Radioactivity of the Hellenic Centre for Marine Research (HCMR) and in the Environmental Radioactivity Laboratory (ERL) of the Institute of Nuclear Technology—Radiation Protection of the National Centre for Scientific Research 'Demokritos' (NCSRD). Samples were prepared according to the methodological guidelines, which were adopted as a part of the project RER/7/003 of the IAEA. According to these guidelines, stones, shells and algae were removed and the weight of the remaining sediment was recorded. Then the sample was homogenised and dried overnight at 105°C until a constant weight. After that, the sample was sieved through a 2-mm sieve, weighed and the weight of dry sample was recorded. Then the material was homogenised and the subsample was taken to obtain the optimal counting geometry.

Hellenic Centre for Marine Research

Activity concentrations of natural radionuclides in sediment samples were measured using a HPGe detector (Ortec Coaxial n-type HPGe Detector

System) with a nominal relative efficiency of 50% and resolution of 1.85 keV at 1.33 MeV. A lead shield surrounded the detector in order to reduce the ambient gamma-ray background.

The energy and efficiency calibration procedures were performed using a ^{152}Eu(93%) + ^{154}Eu(7%) source that had been prepared and calibrated at NCSRD, specifically for this type of measurements, in the following way: a small quantity of ^{152}Eu + ^{154}Eu diluted liquid source (obtained originally from Amersham Co.) was put in a 1.0-ml syringe, placed at a distance of 25 cm from the face of the detector. The activity of this quantity was measured (regarding almost point-source geometry) and then the contents of the syringe were injected-dropped into an inert material (talcum powder) that had been placed inside a plastic container (diameter of 6.9 cm, depth of 2 cm) identical to the ones used for the subsequently measured sediment samples. The empty syringe was measured again in order to determine the activity actually injected-dropped into the inert material. Finally, this newly prepared source was placed in contact geometry in front of the detector and a spectrum was recorded. The source was rotated so that the back face was in contact with the detector's front and a second spectrum was recorded. The difference in the intensities for the two spectra was ~3%, thus ensuring that the distribution of radioactivity in the inert material was almost homogenous. After adding the two spectra and using the most intensive gamma-ray peaks of the source, the absolute detection efficiency along with the energy was determined. The empirical function used for the fit was of the type:

$$y = \frac{Ax^b}{C + x^d} \quad (1)$$

Table 1. ^{238}U series (^{226}Ra, ^{214}Pb and ^{214}Bi) in sediment profiles of station 13A of Amvrakikos Gulf analysed by NCSR 'Demokritos' and HCMR.

Depth (cm) *13A*	^{226}Ra (Bq kg^{-1})	^{214}Pb (Bq kg^{-1}) NCSRD	^{214}Bi (Bq kg^{-1})	^{226}Ra (Bq kg^{-1})	^{214}Pb (Bq kg^{-1}) HCMR	^{214}Bi (Bq kg^{-1})
0.5	17.0 ± 4.3	16.5 ± 1.5	20.2 ± 1.8	22.2 ± 2.3	—	—
1.5	12.1 ± 2.7	10.7 ± 1.5	18.4 ± 1.4	18.2 ± 1.9	12.2 ± 1.1	20.8 ± 1.5
2.5	12.2 ± 2.8	9.8 ± 1.8	14.0 ± 1.9	17.0 ± 1.6	11.1 ± 1.0	19.3 ± 1.7
3.5	10.2 ± 2.2	6.8 ± 1.2	13.9 ± 1.4	14.5 ± 1.6	12.5 ± 1.1	18.3 ± 1.7
4.5	10.9 ± 2.0	9.3 ± 1.8	11.6 ± 1.1	12.6 ± 1.3	14.7 ± 1.2	17.8 ± 1.7
5.5	15.0 ± 1.9	13.6 ± 1.5	10.1 ± 1.9	13.8 ± 1.3	18.7 ± 1.3	14.1 ± 1.4
6.5	13.8 ± 1.7	12.6 ± 1.3	9.3 ± 1.9	14.6 ± 1.4	17.3 ± 1.3	14.6 ± 1.6
7.5	13.4 ± 1.8	10.6 ± 1.8	12.1 ± 1.6	14.8 ± 1.3	15.9 ± 1.2	14.6 ± 1.4
8.5	10.3 ± 1.9	7.3 ± 1.1	14.6 ± 1.0	13.0 ± 1.3	12.0 ± 1.1	17.9 ± 1.8
9.5	11.9 ± 2.1	10.3 ± 1.1	9.3 ± 1.3	12.6 ± 1.3	13.2 ± 1.1	15.3 ± 1.4
10.5	11.6 ± 2.0	9.9 ± 1.3	9.2 ± 1.2	12.2 ± 1.3	15.5 ± 1.2	14.6 ± 1.3
11.5	12.8 ± 1.7	10.5 ± 1.1	11.1 ± 1.9	14.2 ± 1.4	14.3 ± 1.2	15.4 ± 1.4
12.5	13.4 ± 2.0	11.9 ± 1.0	9.6 ± 1.2	13.8 ± 1.6	15.7 ± 1.6	15.9 ± 1.4
13.5	13.6 ± 1.9	10.7 ± 1.1	12.5 ± 1.9	14.6 ± 1.6	11.5 ± 1.0	13.5 ± 1.3
14.5	11.1 ± 1.6	9.2 ± 1.2	9.4 ± 1.1	12.6 ± 1.2	13.4 ± 1.1	12.5 ± 1.2
15.5	12.4 ± 1.6	10.2 ± 1.1	10.7 ± 1.9	14.2 ± 1.4	11.0 ± 1.0	16.2 ± 1.4
16.5	10.0 ± 1.8	8.5 ± 1.5	8.0 ± 1.5	13.4 ± 1.4	17.0 ± 1.3	11.4 ± 1.3
17.5	14.8 ± 2.7	13.6 ± 1.6	9.9 ± 1.7	13.8 ± 1.4	5.7 ± 0.8	6.5 ± 0.9
18.5	13.9 ± 1.7	11.6 ± 1.0	11.6 ± 1.1	13.3 ± 1.3	12.8 ± 1.1	13.6 ± 1.3
19.5	14.5 ± 1.4	13.6 ± 1.8	9.0 ± 1.0	14.4 ± 1.6	14.9 ± 1.2	8.6 ± 0.5
20.5	14.4 ± 1.9	11.8 ± 1.2	12.4 ± 1.5	13.9 ± 1.4	13.5 ± 1.1	9.7 ± 1.1
21.5	10.1 ± 1.5	8.2 ± 1.8	8.8 ± 1.0	13.0 ± 1.4	13.7 ± 1.4	11.6 ± 1.2
22.5	11.6 ± 1.3	9.9 ± 1.7	9.1 ± 1.8	13.3 ± 1.4	12.1 ± 1.0	14.5 ± 1.3
23.5	14.8 ± 1.4	13.7 ± 1.9	9.6 ± 1.9	15.7 ± 1.7	10.3 ± 1.0	15.6 ± 1.7
24.5	14.0 ± 1.6	11.0 ± 1.3	12.9 ± 1.1	14.5 ± 1.6	15.6 ± 1.4	8.6 ± 1.0
26	11.6 ± 1.0	9.6 ± 1.0	9.9 ± 1.3	13.8 ± 1.6	13.7 ± 1.1	12.6 ± 0.4
28	12.7 ± 1.1	10.9 ± 1.5	12.3 ± 1.3	13.4 ± 1.4	14.6 ± 1.2	14.7 ± 2.3
30	12.4 ± 1.0	10.9 ± 1.0	8.9 ± 1.1	13.4 ± 1.4	15.5 ± 1.7	15.8 ± 1.7
32	12.4 ± 0.8	10.5 ± 1.1	10.5 ± 1.3	13.8 ± 1.4	11.2 ± 1.1	11.2 ± 1.1
34	12.5 ± 1.2	9.2 ± 1.0	12.0 ± 1.1	13.0 ± 1.6	8.2 ± 0.7	10.4 ± 0.9
36	13.2 ± 1.0	11.8 ± 1.9	9.6 ± 1.0	13.3 ± 1.4	7.5 ± 0.9	14.2 ± 1.3
38	12.4 ± 0.9	10.8 ± 1.9	9.1 ± 1.1	12.8 ± 1.4	8.3 ± 0.7	12.0 ± 1.2
40	13.1 ± 1.0	10.8 ± 1.8	11.2 ± 1.1	12.6 ± 1.4	13.8 ± 1.1	11.0 ± 0.7

where y is the absolute efficiency, x is the gamma-ray energy and A, b, C and d are the free parameters. In most cases, the measuring time was 24 h, except when the specific activity of a sample was too low and 48-h spectra were recorded. Every 5 d, a 48-h background spectrum was recorded. Concerning the efficiency value at the emission energy of ^{210}Pb (46 keV), a new measurement was performed using an IAEA standard source (IAEA 307).

National Centre for Scientific Research 'Demokritos'

The measurements were carried out in a gamma-spectrometry system comprising an HPGe detector (Canberra Coaxial HPGe Detector System) with a relative efficiency of 90% and resolution of 2.1 keV (at 1.33-MeV photopeak of ^{60}Co). The HPGe detector is connected to a multichannel analyser and the whole system is controlled using specialised software (Canberra Genie 2000). The duration of each measurement was over 7×10^4 s, usually overnight.

The energy calibration was performed using standard active sources of ^{241}Am and ^{60}Co in a range of 2000 keV in 8096 channel spectroscopy (0.25 keV channel^{-1}). The detector's efficiency calibration curve over the gamma-ray energies of interest was derived using a mixed standard solution of ^{241}Am, ^{109}Cd, ^{139}Ce, ^{57}Co, ^{60}Co, ^{137}Cs, ^{203}Hg, ^{113}Sn, ^{85}Sr and ^{88}Y of total activity of 5202 Bq. The mixed standard solution produced photopeaks in the lower energies of the spectrum (specifically ^{241}Am in 59.5 keV and ^{109}Cd in 88.0 keV), where ^{210}Pb emits. As low-energy gamma rays are attenuated quite easily by self-absorption, careful attention must be paid to sample geometry in order to maximise the overall detection efficiency and to ensure reproducibility. Buesseler *et al.*[21] reported that the smaller

Table 2. ^{238}U series (^{226}Ra, ^{214}Pb and ^{214}Bi) in sediment profiles of station 13B of Amvrakikos Gulf analysed by NCSRD and HCMR.

Depth (cm) *13B*	^{226}Ra (Bq kg^{-1})	^{214}Pb (Bq kg^{-1}) NCSRD	^{214}Bi (Bq kg^{-1})	^{226}Ra (Bq kg^{-1})	^{214}Pb (Bq kg^{-1}) HCMR	^{214}Bi (Bq kg^{-1})
0.5	10.9 ± 3.5	9.1 ± 1.9	16.0 ± 2.0	13.5 ± 1.4	16.9 ± 1.2	—
1.5	13.2 ± 2.6	14.2 ± 1.2	12.7 ± 1.4	14.5 ± 1.3	17.3 ± 1.3	—
2.5	15.8 ± 1.8	13.9 ± 1.8	11.8 ± 1.5	14.8 ± 1.5	16.6 ± 1.2	—
3.5	17.3 ± 1.7	14.8 ± 1.4	13.7 ± 1.4	14.9 ± 1.7	18.1 ± 1.3	11.7 ± 1.1
4.5	17.4 ± 1.9	14.7 ± 1.7	13.8 ± 1.1	15.1 ± 1.7	17.9 ± 1.3	10.2 ± 1.1
5.5	17.3 ± 1.5	14.9 ± 1.0	14.8 ± 1.1	14.8 ± 1.5	20.0 ± 1.4	9.8 ± 1.1
6.5	18.2 ± 1.4	16.0 ± 1.9	13.7 ± 2.0	16.5 ± 1.8	18.5 ± 1.3	14.3 ± 1.4
7.5	15.7 ± 1.3	13.4 ± 1.7	12.5 ± 1.8	16.0 ± 1.7	18.9 ± 1.3	16.4 ± 1.7
8.5	17.8 ± 1.2	15.3 ± 1.7	13.7 ± 1.7	16.5 ± 1.7	16.7 ± 1.2	10.1 ± 1.1
9.5	17.4 ± 1.1	14.8 ± 1.7	16.2 ± 1.8	16.8 ± 1.8	20.4 ± 1.4	16.2 ± 1.4
10.5	18.2 ± 1.3	15.1 ± 1.4	13.1 ± 1.6	18.0 ± 2.0	15.1 ± 1.1	19.5 ± 1.6
11.5	15.8 ± 1.3	15.6 ± 1.2	11.4 ± 1.3	17.5 ± 1.8	21.2 ± 1.4	19.6 ± 1.6
12.5	16.2 ± 1.2	15.0 ± 1.6	13.2 ± 1.7	17.2 ± 1.9	19.6 ± 1.3	18.7 ± 1.5
13.5	17.6 ± 1.5	16.4 ± 1.2	14.3 ± 1.3	18.2 ± 1.9	17.8 ± 1.3	16.8 ± 1.4
14.5	16.4 ± 1.4	15.0 ± 1.5	13.9 ± 1.5	17.5 ± 1.8	19.4 ± 1.3	18.3 ± 1.5
15.5	16.0 ± 1.3	14.8 ± 1.9	12.9 ± 1.5	17.0 ± 1.9	21.1 ± 1.5	18.1 ± 1.7
16.5	16.2 ± 1.4	14.9 ± 1.5	13.0 ± 1.6	17.8 ± 1.8	17.1 ± 1.2	19.7 ± 1.7
17.5	16.6 ± 1.4	15.4 ± 1.4	13.5 ± 1.5	17.5 ± 1.9	20.7 ± 1.4	19.9 ± 1.6
18.5	17.6 ± 1.5	16.2 ± 1.5	14.6 ± 1.5	17.5 ± 1.9	18.3 ± 1.3	11.3 ± 1.0
19.5	18.5 ± 1.6	16.8 ± 1.5	15.5 ± 1.6	18.2 ± 2.0	19.4 ± 1.3	18.6 ± 1.5
20.5	11.3 ± 1.0	9.4 ± 1.4	12.8 ± 1.4	13.0 ± 1.5	10.9 ± 1.0	17.4 ± 1.5
21.5	16.3 ± 1.4	15.4 ± 1.4	12.8 ± 1.5	16.0 ± 1.9	18.5 ± 1.4	16.6 ± 1.5
22.5	16.7 ± 1.5	15.5 ± 1.6	12.9 ± 1.6	17.2 ± 1.8	18.7 ± 1.4	18.3 ± 1.7
23.5	16.8 ± 1.4	15.7 ± 1.5	13.7 ± 1.5	17.8 ± 1.8	19.1 ± 1.4	14.8 ± 1.3
24.5	17.4 ± 1.5	16.2 ± 1.1	14.3 ± 1.2	18.0 ± 1.8	19.2 ± 1.4	15.2 ± 1.3
26	16.8 ± 1.4	15.8 ± 1.1	13.7 ± 1.2	17.8 ± 1.8	19.0 ± 1.3	16.9 ± 1.5
28	17.3 ± 1.5	15.9 ± 1.4	12.7 ± 1.4	17.5 ± 1.8	17.0 ± 1.2	15.7 ± 1.4
30	15.2 ± 1.3	13.8 ± 1.1	12.8 ± 1.2	16.5 ± 1.8	17.6 ± 1.3	13.5 ± 1.3
32	15.0 ± 1.3	13.8 ± 1.0	12.1 ± 1.2	16.1 ± 1.8	17.8 ± 1.3	15.2 ± 1.3
34	17.6 ± 1.5	16.4 ± 1.3	14.5 ± 1.2	16.8 ± 1.8	18.1 ± 1.4	16.9 ± 1.5
36	16.6 ± 1.4	15.7 ± 1.2	13.0 ± 1.2	16.5 ± 1.8	17.1 ± 1.2	15.7 ± 1.4
38	16.2 ± 1.4	10.7 ± 1.9	11.2 ± 1.3	16.5 ± 1.8	12.0 ± 1.0	13.5 ± 1.3
40	10.9 ± 3.5	9.1 ± 1.9	16.0 ± 2.0	16.5 ± 1.8	16.9 ± 1.2	14.1 ± 1.4

the sample volume, the higher the detection efficiency. In the present study, the geometry used was of small volume (radius of 3.4 cm and height of 2.0 cm) and efficiency calibration was performed using the same geometry. Due to the small volume, self-absorption of the samples could be assumed negligible. However, the self-absorption of the samples was also checked using a Monte Carlo-based simulation code[22] and was proved insignificant. The quality assurance of the measurements is checked periodically by participating in proficiency tests (e.g. within 2010 ERL has participated in two tests, IAEA-CRP1471-01 proficiency test and an EC inter-laboratory comparison JRC-IRMM).

^{210}Pb sedimentation rate

The excess ^{210}Pb activity concentration with depth was used to calculate the sedimentation rates in the studied area. The excess ^{210}Pb activity concentration is calculated by subtracting the ^{226}Ra activity from the total ^{210}Pb activity concentration. ^{210}Pb is present in the sediments due to background ^{226}Ra activity concentration and due to transported matter that may contain ^{222}Rn daughters. In this case, the sedimentation rates were estimated according to the Constant Flux-Constant Sedimentation model[23]. More specifically, the excess ^{210}Pb activity, $A(z)$, along the sediment core follows the equation:

$$A(z) = A_0 e^{-kz/r} \quad (2)$$

where A_0 is the excess activity concentration in the sediment (Bq kg^{-1}), k is the ^{210}Pb radioactive decay constant (0.03114 y^{-1}), z is the depth of sediment (cm) and r is the sedimentation rate (cm y^{-1}).

The dependence of the logarithmic values of the excess ^{210}Pb activity concentration as a function of depth follows the formula described by Eq. 2. The mean sedimentation rate with the corresponding

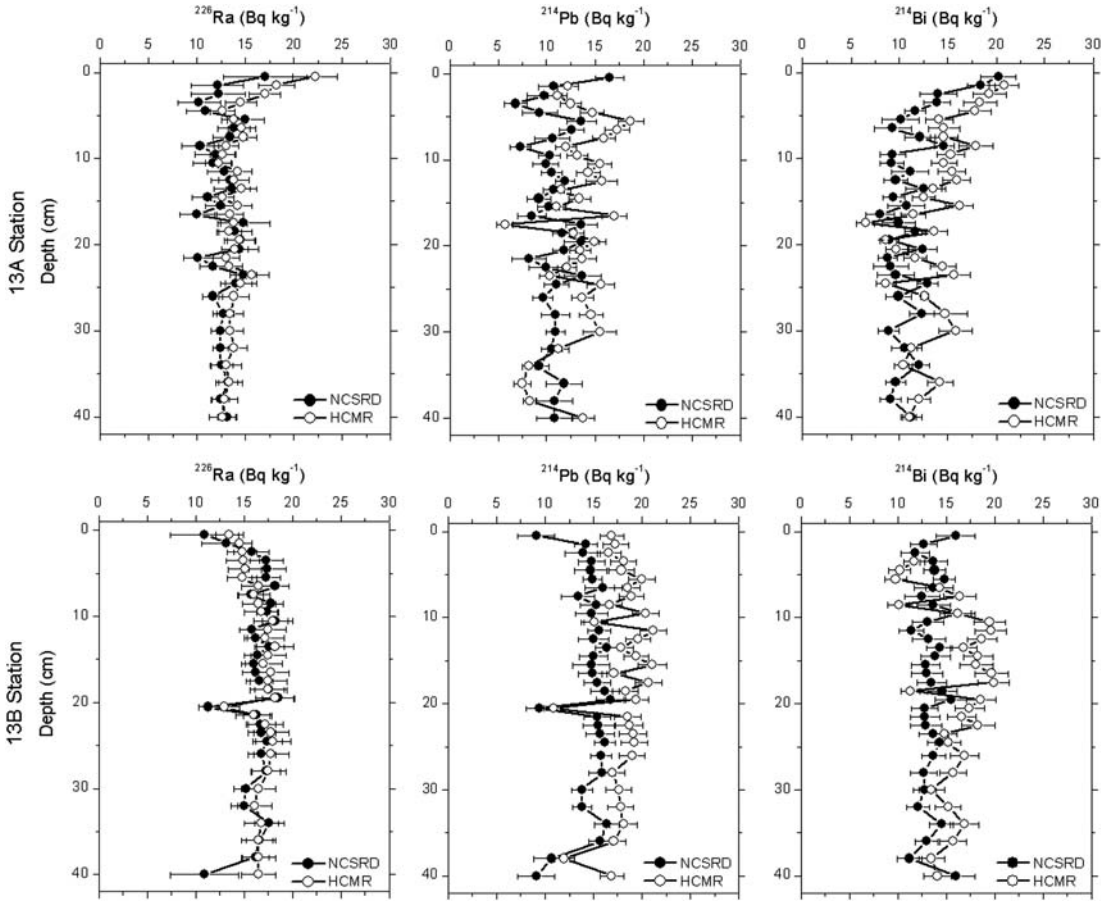

Figure 2. Vertical profiles of ^{238}U daughter concentration activities.

uncertainty is calculated from the slope (k/r) of the fitted line using the least squares fit procedure.

RESULTS

^{238}U series (^{226}Ra, ^{214}Pb and ^{214}Bi)

^{238}U series radionuclides (^{226}Ra, ^{214}Pb and ^{214}Bi) were quantitatively determined in sediment cores of 40 cm depth in two stations (13A and 13B) in the Amvrakikos Gulf (Western Greece). The results obtained by both laboratories (HCMR and NCSRD) are indicated in Tables 1 and 2 and they are also depicted in Figure 2. Although different methodologies were followed by the two laboratories in order to calibrate (energy calibration and efficiency estimation) the detection systems, slight differences were observed. Such differences are more evident regarding ^{222}Rn daughters activity and possible reasons are discussed in detail below. The vertical distribution of ^{226}Ra activity concentration varies from 10 to 22 Bq kg^{-1} and from 11 to 19 Bq kg^{-1} according to stations 13A and 13B, respectively. As concerns ^{222}Rn daughters, their activity concentrations measured in a range from 6 to 22 Bq kg^{-1} in station 13A and from 9 to 21 Bq kg^{-1}in station 13B. Although fluctuations were observed along the depth, the average values of ^{222}Rn daughters (^{214}Pb, ^{214}Bi) activity concentrations (as measured from each laboratory) were found almost equal evidencing that radioactive equilibrium between them has been obtained as expected.

^{232}Th series (^{228}Ac, ^{208}Tl, ^{212}Pb)

^{232}Th series radionuclides ^{228}Ac, ^{212}Pb and ^{208}Tl were quantitatively determined as well. ^{212}Bi is transmuted to ^{208}Tl (35.9%) and to ^{212}Po (64.1%) according to the decay chain of ^{232}Th. Therefore ^{208}Tl

Table 3. ^{232}Th series radionuclides ^{228}Ac, ^{208}Tl and ^{212}Pb in sediment profiles of station 13A of Amvrakikos Gulf analysed by NCSRD and HCMR (^{208}Tl has been normalised).

Depth (cm) *13A*	^{228}Ac (Bq kg^{-1})	^{208}Tl (Bq kg^{-1}) NCSRD	^{212}Pb (Bq kg^{-1})	^{228}Ac (Bq kg^{-1})	^{208}Tl (Bq kg^{-1}) HCMR	^{212}Pb (Bq kg^{-1})
0.5	23.5 ± 5.1	34.6 ± 4.1	22.2 ± 4.6	17.2 ± 4.1	29.0 ± 3.1	23.3 ± 2.1
1.5	17.7 ± 6.6	28.8 ± 5.4	21.2 ± 2.9	18.6 ± 4.1	18.5 ± 1.9	20.7 ± 2.1
2.5	17.7 ± 6.6	16.8 ± 4.5	19.7 ± 2.3	21.6 ± 4.2	18.9 ± 2.2	20.5 ± 2.0
3.5	12.0 ± 5.1	10.8 ± 1.9	14.0 ± 1.6	22.5 ± 5.9	18.7 ± 1.9	20.6 ± 2.0
4.5	14.1 ± 5.0	14.9 ± 2.7	12.7 ± 1.6	15.4 ± 3.7	16.8 ± 1.9	18.6 ± 2.1
5.5	17.5 ± 4.4	16.0 ± 2.4	11.0 ± 1.8	24.3 ± 3.9	14.5 ± 1.8	16.8 ± 1.9
6.5	13.8 ± 4.4	14.5 ± 2.7	11.6 ± 1.9	23.2 ± 4.2	18.3 ± 1.9	16.4 ± 1.9
7.5	14.3 ± 4.3	12.6 ± 2.3	7.6 ± 1.8	22.2 ± 4.3	17.9 ± 1.9	14.9 ± 2.0
8.5	13.0 ± 4.6	9.9 ± 2.7	5.8 ± 1.7	18.0 ± 3.9	17.8 ± 2.0	16.6 ± 1.9
9.5	11.8 ± 5.3	13.5 ± 2.6	11.3 ± 2.1	21.5 ± 4.1	15.2 ± 1.8	17.9 ± 2.4
10.5	15.8 ± 4.7	8.2 ± 2.3	11.4 ± 2.3	22.1 ± 4.4	17.0 ± 1.8	16.6 ± 2.3
11.5	11.2 ± 4.4	8.3 ± 2.0	7.8 ± 1.7	22.2 ± 4.1	18.1 ± 1.9	18.2 ± 2.3
12.5	12.4 ± 5.3	8.8 ± 2.1	9.2 ± 1.6	16.8 ± 4.8	17.2 ± 2.3	17.4 ± 1.9
13.5	15.5 ± 4.7	12.1 ± 2.9	10.0 ± 1.9	13.5 ± 3.0	10.2 ± 1.5	14.1 ± 1.8
14.5	12.6 ± 3.7	12.5 ± 2.8	9.5 ± 2.0	18.1 ± 4.8	9.7 ± 1.3	21.8 ± 2.0
15.5	15.9 ± 3.9	14.4 ± 2.6	12.0 ± 1.9	24.1 ± 6.2	15.3 ± 1.8	20.8 ± 2.1
16.5	12.6 ± 4.5	7.4 ± 3.1	13.6 ± 1.6	7.3 ± 1.0	15.0 ± 1.9	15.0 ± 1.8
17.5	17.7 ± 6.7	14.1 ± 2.0	11.1 ± 1.1	10.6 ± 1.0	9.6 ± 1.4	14.5 ± 2.1
18.5	13.8 ± 4.0	13.5 ± 2.3	10.6 ± 1.5	12.5 ± 1.2	11.3 ± 1.3	14.8 ± 2.9
19.5	17.1 ± 3.4	13.6 ± 2.3	11.7 ± 1.2	13.1 ± 1.3	11.7 ± 1.3	15.1 ± 1.8
20.5	20.2 ± 4.6	14.9 ± 3.1	11.0 ± 1.9	15.2 ± 1.5	11.5 ± 1.3	14.9 ± 1.9
21.5	15.6 ± 3.6	12.0 ± 2.7	11.7 ± 2.0	15.5 ± 1.6	11.1 ± 1.3	14.9 ± 1.9
22.5	15.8 ± 3.0	13.8 ± 2.1	15.2 ± 1.0	16.1 ± 1.6	11.8 ± 1.4	16.1 ± 2.1
23.5	17.5 ± 3.4	15.1 ± 2.3	14.7 ± 1.3	17.2 ± 1.7	12.2 ± 1.4	15.9 ± 2.0
24.5	20.3 ± 3.8	15.5 ± 2.7	15.6 ± 1.6	20.1 ± 2.1	12.5 ± 1.4	17.1 ± 2.3
26	15.0 ± 2.3	14.9 ± 2.6	13.2 ± 1.8	19.5 ± 2.0	12.7 ± 1.4	16.2 ± 2.1
28	16.8 ± 2.9	14.7 ± 3.8	13.4 ± 1.9	18.2 ± 2.0	12.6 ± 1.4	15.8 ± 2.2
30	17.7 ± 2.5	16.9 ± 2.5	13.8 ± 2.1	17.8 ± 1.9	13.3 ± 1.4	15.8 ± 2.2
32	18.7 ± 1.9	16.6 ± 2.3	14.3 ± 2.0	17.1 ± 1.8	13.2 ± 1.4	16.8 ± 2.6
34	18.3 ± 2.8	15.0 ± 2.6	14.3 ± 2.0	16.9 ± 1.8	13.0 ± 1.4	16.9 ± 1.8
36	17.6 ± 2.4	15.8 ± 2.3	16.0 ± 1.9	16.6 ± 1.7	13.5 ± 1.4	18.1 ± 1.8
38	19.9 ± 2.2	17.2 ± 2.2	15.1 ± 1.9	17.1 ± 1.7	13.7 ± 1.4	17.6 ± 2.2
40	17.9 ± 2.4	15.0 ± 2.0	15.0 ± 1.8	17.5 ± 1.7	13.9 ± 1.4	17.1 ± 2.4

activity concentrations were also normalised using the proper branching ratios in the decay scheme in order to compare its activity with those of ^{212}Pb and ^{228}Ac and examine if secular equilibrium occurs. The results are indicated in Tables 3 and 4 and they are also depicted in Figure 3. The vertical distribution of ^{228}Ac concentration shows an almost constant trend, within the uncertainties, along with the depth exhibiting an average activity of 17 ± 3 Bq kg^{-1} and 28 ± 3 Bq kg^{-1} for the stations 13A and 13B, respectively. The activity concentration of ^{220}Rn daughters (^{212}Pb, ^{208}Tl) varies from 6 to 35 Bq kg^{-1} in the station 13A and from 12 to 36 Bq kg^{-1} in the station 13B. Similarly, with ^{222}Rn daughters, the average values of activity concentrations of ^{220}Rn daughters (as measured from each laboratory) were found to be almost equal, indicating that radioactive equilibrium between them has been obtained as expected.

Potassium-40

The results of the activity concentrations of ^{40}K are indicated in Tables 5 and depicted in Figure 4. The measured data from the two laboratories at both stations agreed very well within their uncertainties. The vertical distribution of ^{40}K follows an almost constant trend (with an average values of 420 ± 20 Bq kg^{-1}) for 13A station, while there is a significant increment in the case of 13B station (starting from 500 Bq kg^{-1} at the surface of sediment rising up to a constant value of 730 Bq kg^{-1} at the deeper part of the core). The higher values at 13B station may be attributed to the muddy content and the minerals of the sediment at this location. More particularly, as it has been reported[14], the fraction of sand in the sediment of the region next to the Preveza Strait (13A) is higher than that in the centre of the Gulf (13B) where muddy content is dominant. Similar

Table 4. ^{232}Th series radionuclides ^{228}Ac, ^{208}Tl and ^{212}Pb in sediment profiles of station 13B of Amvrakikos Gulf analysed by NCSRD and HCMR.

Depth (cm) *13B*	^{228}Ac (Bq kg^{-1})	^{208}Tl (Bq kg^{-1}) NCSRD	^{212}Pb (Bq kg^{-1})	^{228}Ac (Bq kg^{-1})	^{208}Tl (Bq kg^{-1}) HCMR	^{212}Pb (Bq kg^{-1})
0.5	19.7 ± 2.1	23.8 ± 7.2	35.8 ± 3.9	21.2 ± 2.2	20.2 ± 2.5	23.5 ± 2.3
1.5	19.6 ± 6.0	26.0 ± 5.1	30.7 ± 2.5	25.4 ± 2.8	21.2 ± 2.5	28.7 ± 2.9
2.5	21.3 ± 4.8	17.5 ± 2.9	20.8 ± 1.5	29.6 ± 3.2	19.8 ± 2.5	16.1 ± 1.8
3.5	22.7 ± 4.0	22.1 ± 2.7	19.7 ± 1.5	31.5 ± 3.5	19.0 ± 3.0	16.8 ± 1.8
4.5	23.0 ± 4.2	21.2 ± 2.3	20.0 ± 1.4	29.7 ± 3.8	15.5 ± 2.6	18.2 ± 2.2
5.5	23.2 ± 3.5	20.9 ± 2.4	20.4 ± 1.2	26.6 ± 2.6	20.6 ± 4.9	18.1 ± 2.8
6.5	23.3 ± 3.6	20.2 ± 2.4	21.4 ± 1.3	20.6 ± 2.2	14.2 ± 3.4	17.4 ± 2.0
7.5	23.8 ± 3.1	18.8 ± 2.2	20.7 ± 1.2	25.2 ± 3.0	19.2 ± 4.5	24.5 ± 2.1
8.5	24.2 ± 3.1	19.4 ± 2.2	22.2 ± 1.2	27.4 ± 3.2	17.2 ± 3.9	27.0 ± 2.8
9.5	27.6 ± 2.7	20.6 ± 2.3	23.1 ± 1.2	28.3 ± 3.2	17.6 ± 3.9	27.2 ± 2.6
10.5	25.0 ± 3.3	24.9 ± 2.9	24.1 ± 1.0	31.3 ± 3.8	16.6 ± 3.7	24.2 ± 2.4
11.5	25.3 ± 2.3	21.4 ± 2.6	21.9 ± 0.9	33.0 ± 3.8	17.2 ± 3.9	25.0 ± 2.7
12.5	28.5 ± 3.0	21.2 ± 2.1	25.4 ± 1.2	35.9 ± 3.6	17.4 ± 4.1	24.1 ± 2.6
13.5	26.2 ± 2.3	23.3 ± 2.6	23.2 ± 0.9	35.7 ± 3.6	17.3 ± 4.0	23.5 ± 2.5
14.5	26.0 ± 2.6	23.9 ± 2.8	23.6 ± 1.0	31.6 ± 3.2	16.7 ± 3.8	24.6 ± 2.5
15.5	27.6 ± 2.7	24.1 ± 2.9	24.8 ± 1.0	31.1 ± 3.2	18.4 ± 4.3	21.9 ± 2.3
16.5	26.0 ± 2.6	23.0 ± 2.8	24.8 ± 0.9	32.2 ± 3.2	16.3 ± 3.7	20.4 ± 2.0
17.5	26.7 ± 3.1	23.4 ± 2.9	24.7 ± 1.3	31.0 ± 3.2	14.4 ± 3.2	21.7 ± 2.3
18.5	28.4 ± 2.8	23.7 ± 2.9	24.8 ± 1.0	31.0 ± 3.4	21.3 ± 4.2	23.7 ± 2.4
19.5	29.1 ± 3.0	24.5 ± 2.1	25.7 ± 1.0	32.0 ± 3.4	19.1 ± 4.5	25.7 ± 2.5
20.5	23.4 ± 2.5	12.2 ± 2.7	13.0 ± 0.8	27.1 ± 3.1	21.0 ± 4.9	16.5 ± 2.7
21.5	27.4 ± 2.6	25.1 ± 2.7	24.6 ± 1.0	27.5 ± 2.9	17.3 ± 4.1	23.9 ± 2.5
22.5	27.2 ± 3.3	25.0 ± 2.9	24.7 ± 1.5	27.8 ± 2.9	17.2 ± 4.0	30.7 ± 3.2
23.5	27.0 ± 2.7	25.1 ± 2.8	25.4 ± 1.0	28.0 ± 2.9	21.5 ± 4.0	31.9 ± 3.2
24.5	26.5 ± 2.2	24.7 ± 2.5	24.1 ± 0.8	27.5 ± 2.8	17.7 ± 4.0	28.8 ± 3.1
26	26.5 ± 2.2	23.0 ± 2.5	24.4 ± 0.8	27.7 ± 2.9	17.9 ± 3.8	27.5 ± 3.1
28	28.1 ± 2.4	25.1 ± 2.6	25.0 ± 0.9	28.2 ± 2.9	18.3 ± 3.8	27.2 ± 3.1
30	26.3 ± 2.2	23.3 ± 2.5	24.5 ± 0.8	27.8 ± 2.9	18.7 ± 3.9	26.9 ± 3.1
32	27.6 ± 2.0	25.3 ± 2.4	24.7 ± 0.7	28.2 ± 3.0	18.2 ± 3.7	27.1 ± 3.1
34	29.0 ± 2.2	23.8 ± 2.5	29.9 ± 0.9	28.5 ± 3.0	17.9 ± 3.7	27.5 ± 3.1
36	28.0 ± 2.1	25.5 ± 2.5	24.8 ± 0.8	29.1 ± 3.0	17.5 ± 3.6	26.7 ± 3.1
38	27.0 ± 2.1	14.5 ± 2.7	15.0 ± 0.8	28.6 ± 3.0	18.3 ± 3.8	20.0 ± 3.0
40	22.9 ± 2.4	15.0 ± 2.0	15.0 ± 1.8	27.0 ± 2.9	17.1 ± 3.5	18.0 ± 2.2

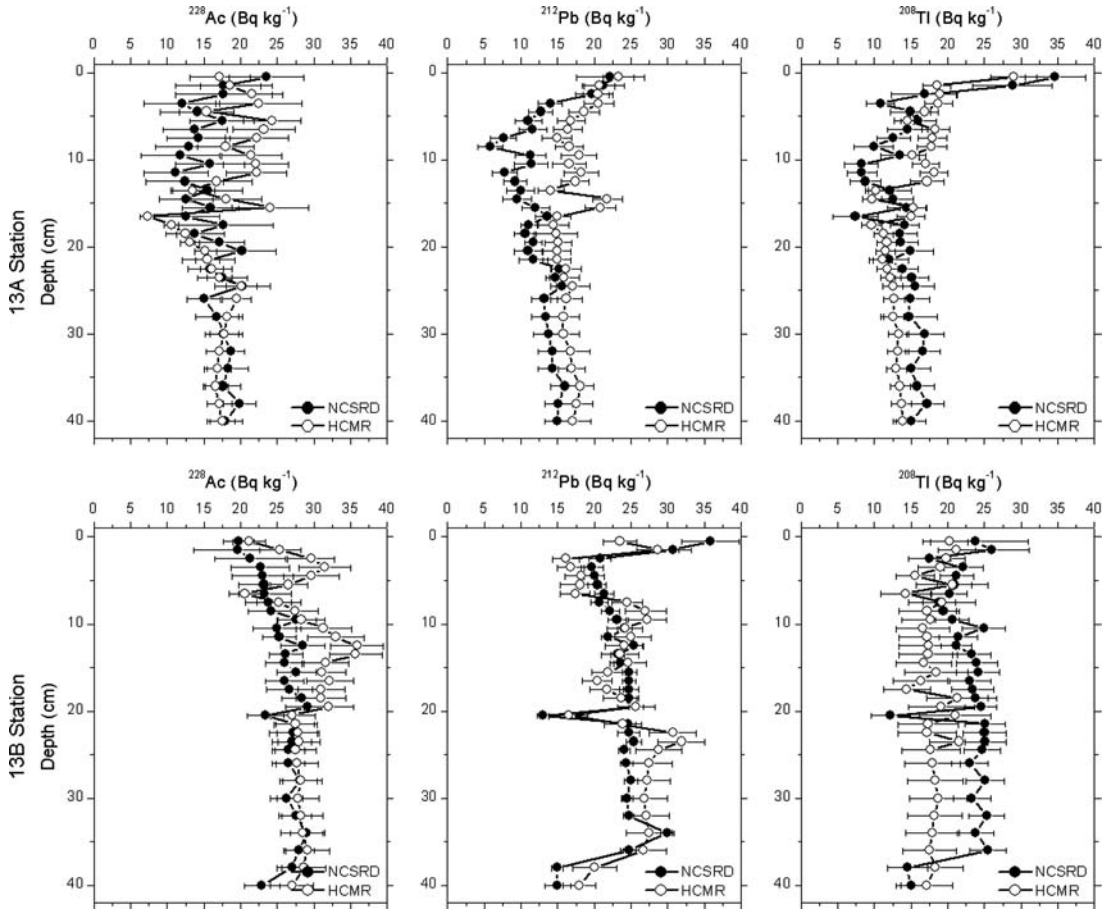

Figure 3. Vertical profiles of ^{232}Th daughter concentration activities.

observations have been reported[5] in another closed system (Butrint Lake) near the Vivari channel. Also there, the activity concentration of ^{40}K was found enhanced in the sediment samples of the lake where the fraction of sand was smaller.

Lead-210

The results of ^{210}Pb measurements are indicated in Table 6 and depicted in Figure 5 for the two stations, respectively. The logarithmic excess ^{210}Pb activity vs. depth was used for the sedimentation rate calculations. The general trend of the vertical distribution of ^{210}Pb follows exponential decrement along the depth for 13B station (starting from 250 to 50 Bq kg^{-1}). At station 13A similar behaviour is observed including significant fluctuations at around 11 and 22 cm. These fluctuations may be attributed to possible depositions that have been taking place during recent years through the transfer of suspended materials in the studied location.

DISCUSSION

No data have been reported in the literature concerning vertical profiles of natural radionuclide concentrations in the specific region; therefore, no comparison is possible. However, the ratio of the averaged daughter concentrations of ^{238}U to ^{232}Th and ^{40}K to ^{232}Th were calculated for the samples of both stations to study any equilibrium processes of natural radionuclides in the core sediments. Additionally, the disequilibrium between ^{210}Pb and ^{226}Ra is also discussed.

^{238}U/^{232}Th, ^{40}K/^{232}Th and ^{210}Pb/^{226}Ra

The ratio of the concentration of ^{232}Th and ^{238}U daughters (^{228}Ac and ^{226}Ra, respectively) was

Table 5. ^{40}K in sediment profiles of stations 13A and 13B of Amvrakikos Gulf analysed by NCSRD and HCMR.

Depth (cm)	Station 13A (Bq kg^{-1}) NCSRD	Station 13B (Bq kg^{-1}) NCSRD	Station 13A (Bq kg^{-1}) HCMR	Station 13B (Bq kg^{-1}) HCMR
0.5	394 ± 46	565 ± 53	—	480 ± 45
1.5	420 ± 31	619 ± 62	412 ± 35	556 ± 48
2.5	458 ± 34	682 ± 66	434 ± 41	590 ± 50
3.5	409 ± 53	718 ± 67	461 ± 43	621 ± 51
4.5	389 ± 46	721 ± 63	445 ± 44	626 ± 52
5.5	438 ± 46	722 ± 74	405 ± 44	686 ± 63
6.5	385 ± 45	718 ± 76	422 ± 45	623 ± 60
7.5	348 ± 35	747 ± 74	407 ± 41	705 ± 69
8.5	359 ± 38	746 ± 74	392 ± 40	825 ± 69
9.5	429 ± 38	739 ± 73	402 ± 40	733 ± 60
10.5	397 ± 38	749 ± 75	410 ± 40	839 ± 51
11.5	423 ± 46	689 ± 70	401 ± 39	819 ± 79
12.5	402 ± 39	776 ± 74	412 ± 40	805 ± 79
13.5	433 ± 47	726 ± 71	410 ± 40	667 ± 65
14.5	393 ± 34	695 ± 72	418 ± 42	697 ± 69
15.5	418 ± 34	727 ± 72	406 ± 39	726 ± 71
16.5	405 ± 38	779 ± 71	415 ± 42	695 ± 68
17.5	441 ± 32	778 ± 72	410 ± 40	641 ± 64
18.5	419 ± 45	775 ± 73	420 ± 43	659 ± 65
19.5	425 ± 43	757 ± 73	420 ± 42	695 ± 69
20.5	431 ± 47	738 ± 80	418 ± 42	794 ± 76
21.5	411 ± 43	747 ± 72	426 ± 43	699 ± 68
22.5	431 ± 42	738 ± 70	419 ± 44	732 ± 71
23.5	453 ± 44	729 ± 72	428 ± 43	768 ± 75
24.5	447 ± 44	735 ± 71	432 ± 41	805 ± 79
26	433 ± 42	726 ± 70	437 ± 41	750 ± 69
28	427 ± 40	692 ± 72	426 ± 41	740 ± 69
30	447 ± 49	703 ± 71	431 ± 41	720 ± 73
32	454 ± 47	733 ± 69	441 ± 45	732 ± 71
34	440 ± 41	721 ± 71	451 ± 41	720 ± 76
36	425 ± 30	702 ± 70	442 ± 42	710 ± 70
38	445 ± 38	728 ± 70	431 ± 42	720 ± 70
40	432 ± 41	632 ± 61	438 ± 44	680 ± 65

calculated for all samples and its values found in a range from 1.5 to 3.As a comparison index, the mean value of the ratio (^{226}Ra/^{228}Ac) was also calculated by a least square fitting (see Figure 6a) and it was found equal to 2.5 with a correlation coefficient of $R^2 = 0.70$. Considering that secular radioactive equilibrium exists between ^{238}U/^{226}Ra and ^{232}Th /^{228}Ac, this value (^{226}Ra/^{228}Ac) was compared and found to be <3.3, which has been reported[24] as the world average ratio of ^{238}U/^{232}Th. Also, this ratio indicates that the TENORM contribution from human activities could be considered negligible.

Similarly, correlations between ^{40}K and ^{232}Th were also realised. The measurements of ^{40}K and ^{228}Ac activity concentrations were linearly fitted and depicted in Figure 6b where a significant correlation was observed ($R^2 = 0.86$). The results indicate that there is a positive correlation between activities of ^{40}K and ^{228}Ac (daughter nuclei of ^{232}Th in secular equilibrium). So, from the slope of the linear fit the mean value of the ratio of ^{40}K/^{232} Th was found to be equal to 25. This value is comparable with a neighbouring region in the Gulf of Patras[25] where the ratio of ^{40}K/^{232}Th varied from 16 to 21 for all sample stations.

Regarding the ratio of ^{210}Pb/^{226}Ra (which are both daughters of ^{238}U), a significant disequilibrium was found. More specifically, this ratio ranged between 10 and 20 and is comparable with values reported in the literature for closed and semi-closed marine ecosystems[26].

Sedimentation rate using ^{210}Pb model

Moreover, the mean sedimentation rates (r) were derived using the excess ^{210}Pb data of Table 6. The calculated slope parameter (k/r as given in Eq. 2)

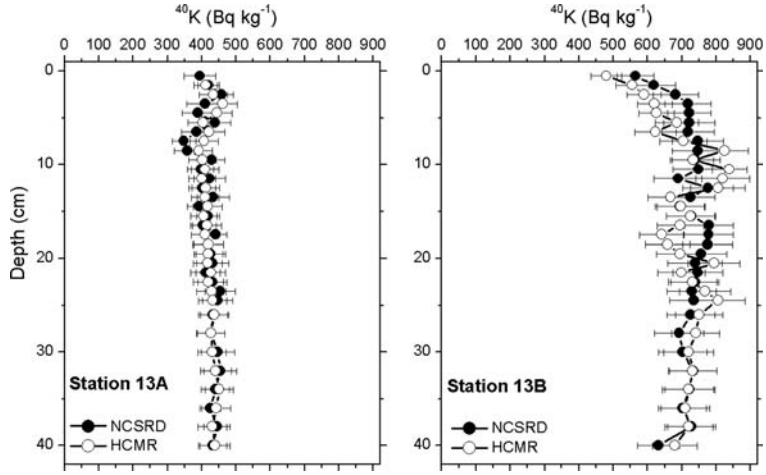

Figure 4. Vertical profiles of ^{40}K concentration activities.

Table 6. ^{210}Pb in sediment profiles of stations 13A and 13B of Amvrakikos Gulf analysed by NCSRD and HCMR.

Depth (cm)	Station 13A (Bq kg^{-1}) NCSRD	Station 13B (Bq kg^{-1}) NCSRD	Station 13A (Bq kg^{-1}) HCMR	Station 13B (Bq kg^{-1}) HCMR
0.5	286 ± 24	242 ± 19	—	—
1.5	306 ± 30	229 ± 18	277 ± 27	212 ± 35
2.5	290 ± 28	224 ± 17	358 ± 35	236 ± 21
3.5	295 ± 29	220 ± 16	352 ± 34	213 ± 21
4.5	291 ± 28	183 ± 14	359 ± 34	158 ± 16
5.5	215 ± 26	154 ± 11	344 ± 33	171 ± 17
6.5	159 ± 11	122 ± 10	215 ± 21	149 ± 15
7.5	166 ± 11	84 ± 9	228 ± 22	132 ± 13
8.5	170 ± 11	76 ± 8	228 ± 32	111 ± 11
9.5	194 ± 21	73 ± 8	229 ± 22	121 ± 12
10.5	165 ± 12	71 ± 8	291 ± 31	67 ± 7
11.5	282 ± 21	72 ± 7	301 ± 29	63 ± 7
12.5	228 ± 23	53 ± 6	310 ± 30	53 ± 6
13.5	198 ± 19	49 ± 5	260 ± 25	67 ± 7
14.5	181 ± 18	34 ± 4	245 ± 24	51 ± 6
15.5	168 ± 17	33 ± 4	264 ± 26	67 ± 7
16.5	165 ± 16	26 ± 4	227 ± 22	61 ± 6
17.5	179 ± 18	36 ± 4	185 ± 18	44 ± 5
18.5	182 ± 18	35 ± 4	250 ± 24	59 ± 6
19.5	180 ± 18	34 ± 4	196 ± 19	46 ± 5
20.5	220 ± 11	33 ± 4	257 ± 25	75 ± 8
21.5	176 ± 17	26 ± 2	293 ± 29	53 ± 6
22.5	175 ± 17	27 ± 3	223 ± 22	61 ± 7
23.5	179 ± 17	34 ± 4	267 ± 26	51 ± 6
24.5	190 ± 18	31 ± 2	258 ± 25	60 ± 6
26	144 ± 14	35 ± 4	225 ± 22	56 ± 6
28	127 ± 13	29 ± 3	193 ± 19	52 ± 6
30	125 ± 12	24 ± 3	176 ± 17	63 ± 7
32	120 ± 12	18 ± 2	148 ± 15	54 ± 6
34	15 ± 2	20 ± 3	126 ± 13	45 ± 5
36	13 ± 1	19 ± 2	29 ± 3	59 ± 6
38	11 ± 1	19 ± 2	33 ± 4	52 ± 6
40	12 ± 1	19 ± 2	18 ± 2	11 ± 1

provides the mean sedimentation rate using the logarithmic representation of the ^{210}Pb data along depth and its decay constant (k). The values of sedimentation rates were estimated to be 0.55 ± 0.02 and 0.32 ± 0.02 cm y^{-1} for the stations 13A and 13B, respectively. The significant difference between the two stations is due to the fact that 13A station is very close to the Preveza Straits where a developed front due to the outflow brackish water of the Gulf and the inflowing saline open sea water has been observed[9]. The saline water inflow transports sediment material from the open sea resulting in variation of the seafloor morphology close to Preveza Straits.

Intercomparison exercise

It is important for the national authorities responsible for radioprotection assessments to obtain reliable data from collaborative laboratories. As both institutes belong to the same national network, which provides data to Greek Atomic Energy Commission, intercomparison exercises contribute to the quality of the assessments. During this study, such an exercise was carried out involving the instrumentation of HCMR and NCRSD laboratories to analyse samples from different cores obtained by same stations. The correlation between the results of the two laboratories shows a good agreement (>90%) for ^{40}K, ^{210}Pb, ^{226}Ra and ^{228}Ac. The discrepancy of the measured data between the two laboratories concerning radon (^{222}Rn) and thoron (^{220}Rn) daughters (^{214}Pb, ^{214}Bi and ^{208}Tl) is attributed to the diffusion of the aforementioned gases inside the sediment of the cores, slightly affecting the spatial activity concentration of their daughters.

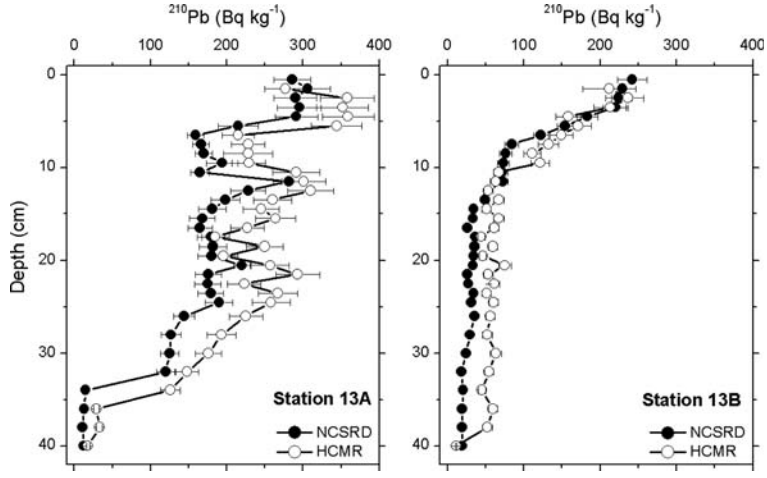

Figure 5. Vertical profiles of ^{210}Pb concentration activities.

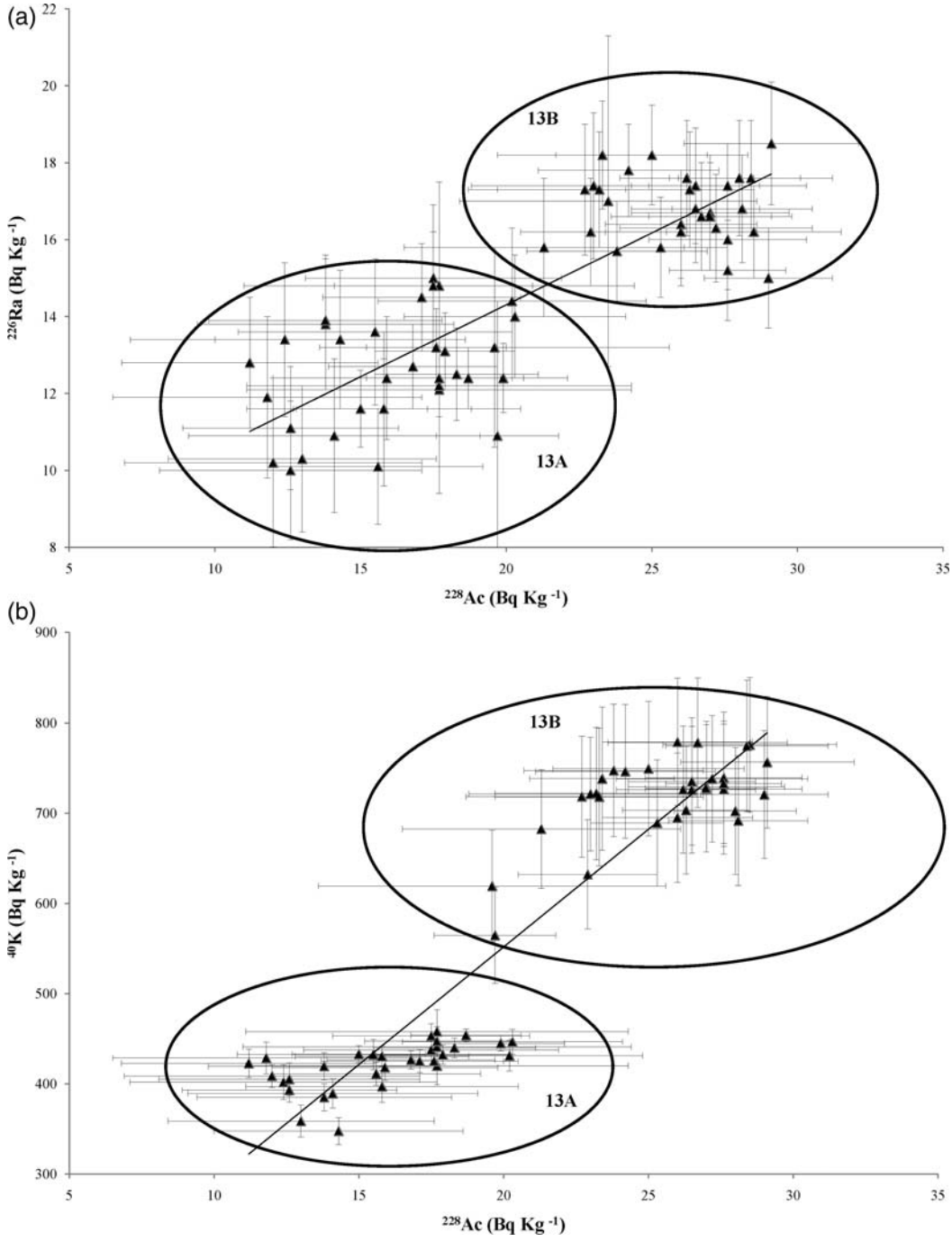

Figure 6. Correlation of (**a**) ^{226}Ra vs. ^{228}Ac activity concentration and (**b**) ^{40}K vs. ^{228}Ac activity concentration.

SUMMARY

In the present work, a comprehensive study of the distribution of gamma-emitting radionuclides in sediment cores from the Amvrakikos Gulf was carried out. The results constitute the first database for natural radioactivity in the specific area. As concerns the activity concentrations of both stations, the measured values do not exceed the recommended limits for ^{226}Ra, ^{40}K and ^{228}Ac. The averaged measured activities between ^{238}U and ^{232}Th daughters are in agreement with measurements reported in the literature indicating that the TENORM contribution from human activities could be considered negligible. The sedimentation rate of the semi-closed Gulf is higher at the Western part of the Gulf (Preveza Straits) than those in the central region. This difference is attributed to the transportation of sediment material by the inflow of Ionian Sea waters into the station 13A. Intercomparison exercises were also carried out exhibiting a good agreement between the results of the two laboratories. This agreement testifies the reliability of the different calibration procedures (for the gamma-ray spectrometry method) in core sediment samples.

ACKNOWLEDGEMENTS

The authors would like to thank Dr Iolanda Osvath for supporting the activities of this work, the staff of the research vessel 'Palagruza' and the organisers for the technical support during the cruise.

FUNDING

The authors would like to thank the IAEA for the financial support of the campaign within the RER/7/003 project.

REFERENCES

1. Matishov, D. G. and Matishov, G. G. *Radioecology in Northern European Seas*. Springer, p. 335 (2004).
2. IAEA. *Naturally occurring radioactive material NORM V*. In: Proceedings of an International Symposium, Seville, Spain, 19–22 March (2007).
3. El-Reefy, H. I., Sharshar, T., Elmimr, T. and Badran, H. *Distribution of gamma-ray emitting radionuclides in the marine environment of the Burullus Lake: II. Bottom sediments*. Environ. Monit. Assess. (2003). doi:10.1007/s10661-009-1169-1.
4. Ababneh, Z. Q., Al-Omari, H., Rasheed, M., Al-Najjar, T. and Ababneh, A. M. *Assessment of gamma-emitting radionuclides in sediment cores from the Gulf of Aqaba. Red Sea*. Radiat. Prot. Dosim. **141**, 289–291 (2010).
5. Tsabaris, C., Eleftheriou, G., Kapsimalis, V., Anagnostou, C., Vlastou, R., Durmishi, C., Kedhi, M. and Kalfas, C. A. *Radioactivity levels of recent sediments in the Butrint Lagoon and the adjacent coast of Albania*. Appl. Radiat. Isot. **65**, 445–453 (2007).
6. Cho, Y. H., Jeong, C. H. and Hahn, R. S. *Sorption characteristics of 137Cs onto clay minerals: effect of mineral structure and ionic strength*. J. Radioanal. Nucl. Chem. **204**, 33–43 (1996).
7. Tsangaris, C., Cotou, E., Papathanassiou, E. and Nicolaidou, A. *Assessment of contaminant impacts in a semi-enclosed estuary (Amvrakikos Gulf, NW Greece): bioenergetics and biochemical biomarkers in mussels*. Environ. Monit. Assess. **161**, 259–269 (2010).
8. Kormas, K. A., Nicolaidou, A. and Reizopoulou, S. *Temporal variations of nutrients and chlorophyl a and particulate matter in three coastal lagoons of Amvrakikos Gulf (Ionian Sea, Greece)*. Mar. Ecol. **22**, 201–213 (2001).
9. Ferentinos, G., Papatheodorou, G., Geraga, M., Iatrou, M., Fakiris, E., Christodoulou, D., Dimitriou, E. and Koutsikopoulos, C. *Fjord water circulation patterns and dysoxic/anoxic conditions in a Mediterranean semi-enclosed embayemnt in the Amvrakikos Gulf, Greece*. Estuar. Coast. Shelf Sci. **88**, 473–481 (2010).
10. Friligos, N. and Balopoulos, E. *Water mass characteristics and degree of eutrophication in a shallow water embayment of the Ionian Sea: Amvrakikos Gulf*. Rapp. Comm. Int. Mer Médit. **31**(2), 56 (1988).
11. Panagiotidis, P. and Florou, H. *Copper, cadmium and iron in marine organisms in a eutriphic estuarine area (Amvrakikos Gulf, Ionian Sea, Greece)*. Toxicol. Environ. Chem. **3–4**, 211–219 (1994).AQ
12. Poulos, S. and Chronis, G. *The importance of the Greek river systems in the evolution of the Greek coastline*. Transformations and Evolution of the Mediterranean Coastline. In: Briand, F. and Maldolado, A., Eds. CIESM Science Series No. 3, Bulletin del' Institut Oceanographique, Monaco, no. 18, pp. 75–96 (1997).
13. Voutsinou-Taliadouri, F. and Balopoulos, E. T. *Geochemical and physical oceanographic aspects of the Amvrakikols Gulf (IonianSea, Greece)*. Toxicol. Environ. Chem. 31–32, 177–185 (1991).
14. Poulos, S. E., Kapsimalis, V., Tziavos, C. and Paramana, T. *Origin and distribution of surface sediments and human impacts on recent sedimentary processes. The case of the Amvrakikos Gulf (NE Ionian Sea)*. Cont. Shelf Res. **28**, 2736–2745 (2008).
15. Tsimplis, M. N. *Tidal oscillations in the Aegean and Ionian seas*. Estuar. Coast. Shelf Sci. **3**, 201–208 (1994).
16. Gotsis-Skreta, O., Psochiou, E., Lempesis, G., Brampa, D., Theodorou, D. and Balopoulos, E. *Seasonal variation of phytoplankton and environmental parameters in a semi-enclosed sea basin, Amvrakikos Gulf, Ionian Sea*. In: Proceedings of the Sixth Hellenic Symposium on Oceanography and Fisheries, vol. 1, Chios, Greece, pp. 512–516 (2000).
17. Poulos, S.E. *Deltaic sedimentation in the microtidal environment of Greek Waters*. Unpublished Ph.D. Thesis, University of Wales, UK, p. 434 (1989).
18. Marinos, G., Stournaras, G. and Karotsieris, Z. *A detailed study on the combined utilisation of the water resources of the rivers Louros and Aracthos drainage basins*. Technical Report to the Ministry of Energy and Natural Resources, Athens (1984).

19. Panayotidis, P., Pancucci, M. A., Balopoulos, E. and Gotsis-Skretas, O. *Plankton distribution patterns in a Mediterranean dilution basin: Amvrakikos Gulf (Ionian Sea, Greece)*. Mar. Ecol. **15**(2), 93–104 (1994).
20. Barnett, P. R. O., Watson, J. and Connelly, D. *A multiple corer for taking virtually undisturbed samples from shelf, bathyal and abyssal sediments*. Oceanol. Acta **7**, 399–408 (1984).
21. Buesseler, K. O., Cochran, J. K., Bacon, M. P., Livingston, H. D., Casso, S. A., Hirschberg, D., Hartman, M. C. and Fleer, A. P. *Determination of thorium isotopes in seawater by non-destructive and radiochemical procedures*. Deep-Sea Res. I **39**, 1103–1114 (1992).
22. Cornejo Díaza, N. and Jurado Vargas, M. *DETEFF: an improved Monte Carlo computer program for evaluating the efficiency in coaxial gamma-ray detectors*. Nucl. Instrum. Methods A **586**, 204–210 (2008).
23. Goldberg, E. G. *Geochronology with ^{210}Pb in Radioactivity Dating*. International Atomic Energy Agency, pp. 121–131 (1963).
24. Adams, J. A. S. *Radioactivity in the lithosphere*. In: Nuclear Radiation in Geophysics. Israel, H. and Krebs, A., Eds. Springer-Verlag (1952).
25. Papaefthymiou, H. V., Chourdakis, G. and Vakalas, J. *Natural radionuclides content and associated dose rates in fine-grained sediments from Patras-Rion sub-basins, Greece*. Radiat. Prot. Dosim. **143**, 117–124 (2011).
26. Brenner, M., Schelske, C. L. and Kenney, W. F. *Inputs of dissolved and particulate ^{226}Ra to lakes and implications for ^{210}Pb dating recent sediments*. J. Paleolimnol. **32**, 53–66 (2004).